The *para*-Didehydropyridine, *para*-Didehydropyridinium, and Related Biradicals—A Contribution to the Chemistry of Enediyne Antitumor Drugs

ELFI KRAKA, DIETER CREMER

Department of Theoretical Chemistry, Göteborg University, Reutersgatan 2, S-41320 Göteborg, Sweden

Received 8 October 1999; accepted 2 August 2000

ABSTRACT: Structure and stability of seven singlet (S) biradicals formed by Bergman cyclization from enediynes are investigated with unrestricted DFT using B3LYP/6-31G(d,p) and B3LYP/6-311+G(3df,3pd). The corresponding triplets (T) are also calculated and compared with their S states utilizing the on-top pair density and the S-T difference on-top pair density. A relationship between the geometry of a S biradical, its stability, and its biradical character is established using the on-top pair density and calculated S-T splittings. Through-bond coupling between the single electrons of the S biradical can be enhanced by the incorporation of a N atom into *para*-didehydrobenzene **1** due to lowering of antibonding orbitals, shortening of ring bonds by anomeric effect, and increased overlap between the interacting orbitals. Strong through-bond interactions lead to a stabilization of the S state and an increase of the S-T splitting. Because through-bond interactions also determine the degree of coupling between the single electrons, stabilization of the S biradical, and an increase of the S-T splitting always means a lowering of the biradical character and the H abstraction ability, which is relevant for the use of N-containing enediynes and their biradicals in connection with the design of new antitumor drugs. The S *para*-didehydropyridine biradical **2** is strongly stabilized and, therefore, has only reduced biradical character. However, the latter can be enhanced by protonation, because this always leads to a lengthening of ring bonds and a reduction of the overlap between interacting orbitals. In the weakly acidic medium of a tumor cell, S biradicals containing an amidine group can be protonated to yield S biradicals with high biradical character (low S-T splittings, small changes in bond alternation relative to the T state), which will abstract H atoms from the DNA of a tumor cell. J Comput Chem 22: 216–229, 2001

Keywords: para-didehydrobenzene; para-didehydroheterobenzenes; DFT-on-top pair density; S-T splitting; Bergman cyclization

Correspondence to: E. Kraka; e-mail: kraka@theoc.gu.se
Contract/grant sponsor: Swedish Natural Science Research Council (NFR)

Introduction

Singlet (S) didehydrobenzene biradicals play an important role in connection with the biological activity of naturally occurring enediynes.[1] The latter contain a delivery system, mostly formed by a polysaccharide rest, a trigger device, and a warhead identical to the enediyne part. The delivery system helps the enediyne to dock into the minor grove of a DNA double strand. By activation of the trigger device, a Bergman cyclization[2] of the enediyne warhead takes place, and a derivative of the *para*-didehydrobenzene in its S state (**1S**, Scheme 1) is formed, which is positioned in such a way in the minor grove of the DNA strands that it can abstract two H atoms, one from each strand of the DNA, to form a more stable arene. This damage of the DNA leads to cleavage along both strands, resulting in cell death. In view of the biological activity of naturally occurring enediynes, present research efforts concentrate on the design of antitumor drugs based on the generation of DNA attacking biradicals from suitable enediynes.[1]

Naturally occurring enediynes are mostly toxic, because they attack both normal and tumor cells.[3] Therefore, it is desirable to design enediyne antitumor drugs that can distinguish between normal and tumor cells. Since the pH value of a tumor cell (6.5–7) is slightly lower than that of a normal cell (7.5), and can be even lowered to a value of 5.5 by invoking hyperglycemia,[4] it has been suggested to start from heteroenediynes that are biologically inactive in the neutral medium of the normal cell but, after protonation in the weakly acidic medium of the tumor cell, gain the typical activity of naturally occurring enediynes. Chen and coworkers[5] investigated for this purpose (Z)-3-aza-hex-3-ene-1,5-diyne, the corresponding biradical *para*-didehydropyridine (**2**, Scheme 1), and its protonated counterpart *para*-didehydropyridinium ion **3** (Scheme 1). Also, biradicals containing an amide group such as **4** (Scheme 1) were suggested as suitable heterobiradicals that can abstract H atoms from DNA if formed from a suitable enediyne.[5]

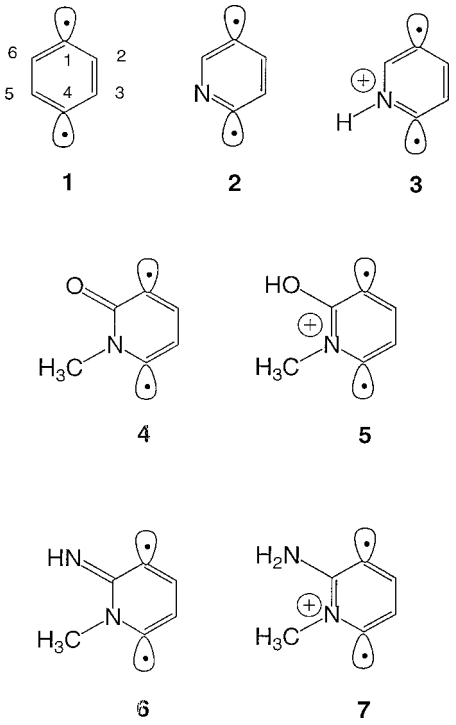

SCHEME 1.

Experimental work on biradicals such as **1S** or **2S** is difficult because of the reactivity of the compounds. Nevertheless, **1S** could be trapped in the matrix at low temperatures and spectroscopically characterized.[6] Biradicals **2S** and **3S** were not found at low temperatures, despite extensive efforts.[5,7] Because of this, information on biradicals such as **1S**, **2S**, or **3S** has to be obtained from reliable quantum chemical investigations.[6,8–14]

Because of the present interest in biradicals containing N, we investigated the S and the triplet (T) state of biradicals **1**–**7** shown in Scheme 1, which can be formed by Bergman cyclization of enediynes **8**–**14** of Scheme 2. In view of the weakly acidic medium of the tumor cell, we concentrated on the change in the properties of N-containing biradicals upon protonation. As suitable reference biradical, we used **1**, that is formed by cyclization of (Z)-hex-3-ene-1,5-diyne **8** (reaction (1a): X = CH, Y = H, see Scheme 3).

The goal of this work is to show how the electronic character and the reactivity (with regard to H abstraction) of a biradical can be assessed from its structural features. For this purpose, we will focus in particular on interactions between the single electrons either by a through-space or through-bond mechanism.[15] Our first investigation of biradical **1S** was carried out at the CCSD(T) level of theory[8] in connection with a reliable determination of the energetic of the Bergman reaction.[16] However, in this work we will use for reasons of feasibility and computational cost density functional theory (DFT). Because it is not obvious that DFT is a suitable method to describe multireference systems such as S biradicals, we will proceed by first discussing the usefulness of DFT in the present work in the next section. Then in the following section we will

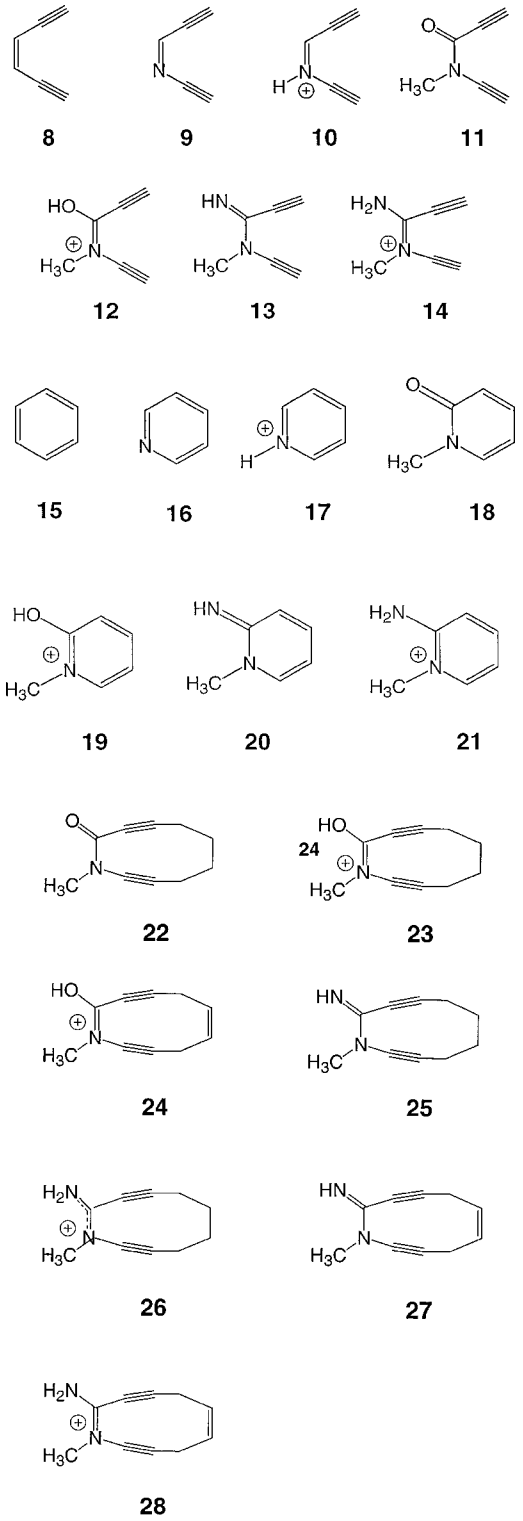

SCHEME 2.

present calculated geometries and S-T splittings for **1**–**7**. In addition, we will use formal reactions shown in Scheme 3 in connection with suitable reference molecules **8**–**21** of Scheme 2 to assess the relative stability of **1**–**7**. Conclusions will be drawn, which of the biradicals investigated in this work, should have the highest H abstraction power and, accordingly, presents a promising candidate in connection with the corresponding enediyne (Scheme 2) for a new antitumor drug.

Is DFT Capable of Describing Singlet Biradicals?

In view of the multireference character of a S biradical, one can expect that only a method covering both static and dynamic electron correlation effects can describe biradicals **1**–**7** correctly. However, MR-CID or MR-AQCC are far too costly to be applied in an investigation of a larger number of biradicals with six or even more heavy atoms. This holds also for CCSD(T),[17] BD(T),[18] or other single determinant methods that cover higher order correlation effects and that have, despite their single determinant character, a chance of providing reasonable descriptions of multireference systems. On the other hand, methods such as CASSCF or CASSCF-PT2[19] do not provide sufficient accuracy, as was documented by various authors.[11, 12] In previous work, we showed that unrestricted DFT (UDFT) performs surprisingly well in the case of singlet biradicals.[6, 20] This was also found by Cramer and coworkers,[12] who noted that UDFT improves the geometry of biradicals such as **1S**–**3S**, and who also provided arguments as to the performance of UDFT in these cases. Actually, UDFT leads to symmetry breaking of the KS ground state of the S biradical because of a mixing of the ground state with the lowest T state. The $\langle \hat{S}^2 \rangle$ value obtained with the KS wave function for the S state is typically close to 1, where this value is erroneous (because it is calculated with the KS determinant) and possesses a doubtful diagnostic value, as was recently shown by Gräfenstein and Cremer.[21] Spin contamination (mixing of S and T states) in the unrestricted description of a S biradical has different consequences for UDFT and UHF. While for UHF symmetry breaking and spin contamination leads to the wrong wave function and a poor description of the corresponding molecule, the electron density is less sensitive to spin contamination and, therefore, properties such as energy or geometry calculated with the help of the electron density rather than the wave function can adopt reasonable values, as was shown by Gräfenstein and coworkers in the case of biradical **1S**.[20] (For prob-

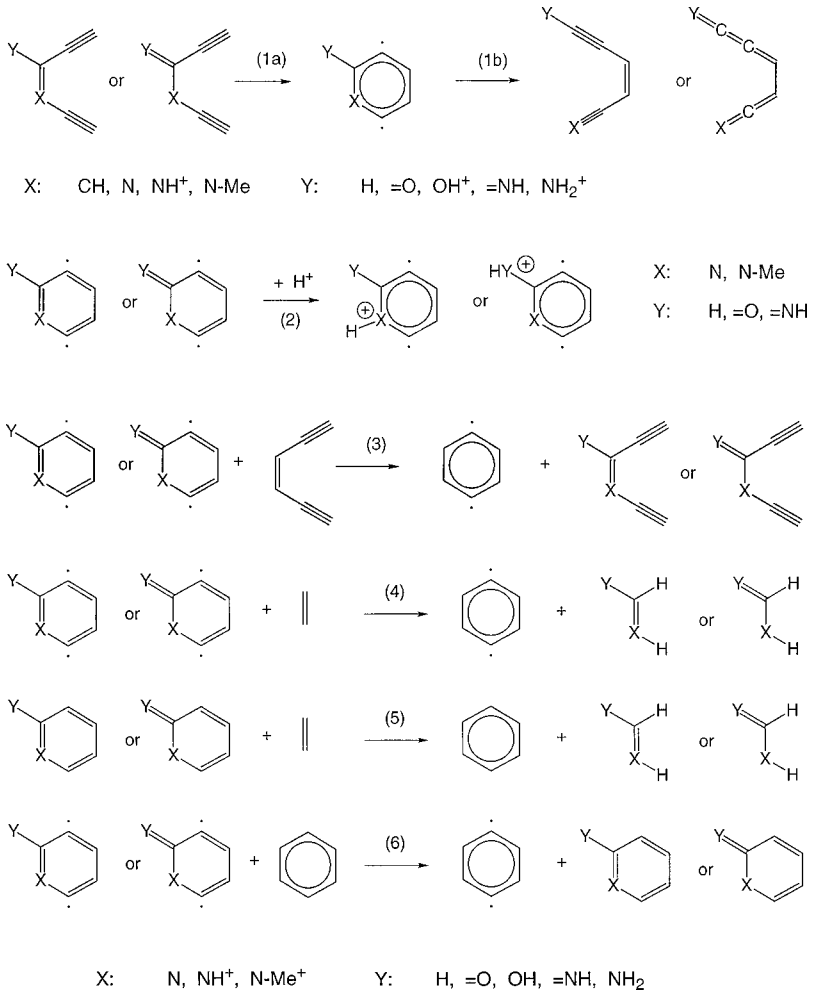

SCHEME 3.

lems in connection with UDFT descriptions, see also refs. 22 and 23.)

Perdew, Savin, and Burke[24] showed that one can ignore the symmetry-breaking problem of UDFT by focusing on the total density $\rho(\mathbf{r})$ and the on-top pair density $P(\mathbf{r},\mathbf{r})$ rather than KS orbitals or spin densities $\rho_\alpha(\mathbf{r})$ and $\rho_\beta(\mathbf{r})$, which should be considered as intermediate quantities without any physical meaning. The on-top pair density $P(\mathbf{r},\mathbf{r})$ is given by the probability of finding two electrons at the same position $\mathbf{r}$ where, in the case of using KS orbitals, $P(\mathbf{r},\mathbf{r})$, $\rho_\alpha(\mathbf{r})$, and $\rho_\beta(\mathbf{r})$ are related by eq. (1):

$$P(\mathbf{r},\mathbf{r}) = 2\rho_\alpha(\mathbf{r})\rho_\beta(\mathbf{r}) \quad (1)$$

The UDFT results are preferably analyzed on the basis of the calculated total density and the on-top density, which contrary to spin densities and KS wave function comply with the symmetry of the molecule.[20, 24] This is a valid approach as long as one does not consider magnetic properties or other quantities directly dependent on the spin densities. In this connection it is noteworthy that the energy can always be expressed as a function of total and on-top pair density.

Figure 1 gives the on-top density distribution $P(\mathbf{r},\mathbf{r})$ for the S state of biradical **1** (Fig. 1a) and the difference on-top density $P(\mathbf{1S}) - P(\mathbf{1T})$ (Fig. 1b) in the form of contour line diagrams as calculated with eq. (1) at the UB3LYP/6-31G(d,p) level of theory. In the case of Figure 1b, solid contour lines indicate that the on-top density is larger in the S, dashed contour lines larger in the T state. Actually, the on-top pair densities of S and T are similar, the differences being about a factor 1000 smaller than the original pair densities. The S state possesses slightly higher on-top densities in the regions of the unpaired electrons (C1 and C4) and in the regions of the in-plane π-orbitals of bonds C2C3 and C5C6. However, along the CC and CH bonds, the T state

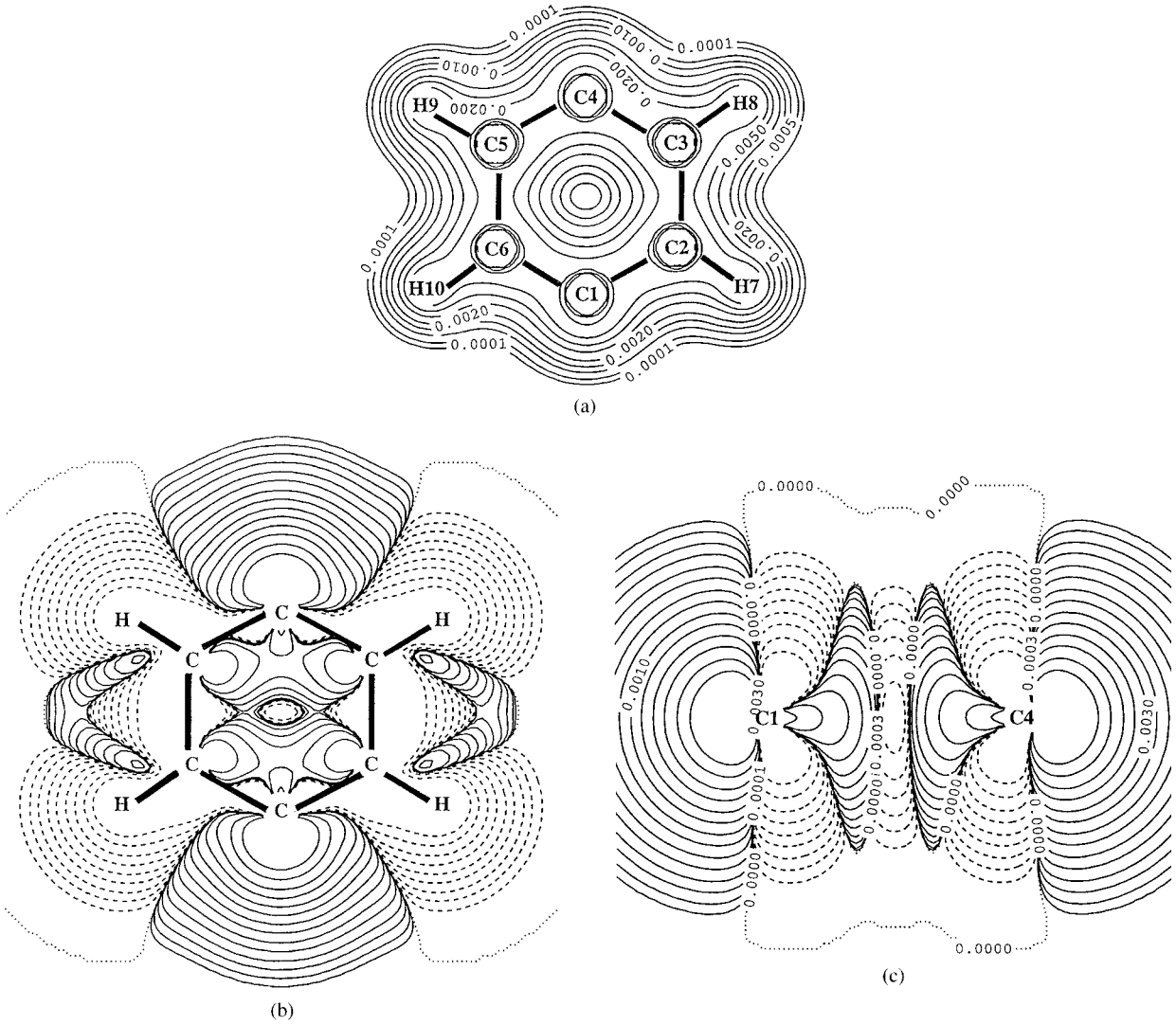

FIGURE 1. (a) UB3LYP/6-31G(d,p) on-top pair density distribution $P(\mathbf{r},\mathbf{r})$ given in the form of a contur line diagram in the plane of **1S**. (Contur lines: 0.0001, 0.0002, 0.0005, 0.001, 0.002, 0.005, 0.01, 0.02, 0.05, 0.1, 0.2 e/bohr^3). (b and c) Contur line diagram of the difference on-top pair density distribution $\Delta P(\mathbf{r},\mathbf{r}) = P(\mathbf{2S}) - P(\mathbf{2T})$ calculated at the UB3LYP/6-31G(d,p) level of theory (b) for the molecular plane and (c) for the plane perpendicular to the molecular plane and passing through nuclei C1 and C4. Solid lines indicate a higher value for the S state, dashed lines, a higher value for the T state, the dotted line indicates equal values for both states. The geometry of **1S** was used. (Contur lines: 0, $\pm 3 \times 10^{-7}$, $\pm 10^{-6}$, $\pm 3 \times 10^{-6}$, $\pm 10^{-5}$, $\pm 3 \times 10^{-5}$, $\pm 10^{-4}$, $\pm 3 \times 10^{-4}$, $\pm 10^{-3}$ e/bohr^3).

has the higher on-top densities (Fig. 1b). This pattern can be understood considering the possibilities of electron delocalization in S and T state. For the S state, there is a small probability of finding the β single electron at the position of the α single electron, while this probability is zero for two single electrons with the same spin in the T state. Through-space coupling between the two single electrons in the S-state would increase the on-top density in the ring center relative to that of the T state. Because this is not the case (Fig. 1c), one can exclude through-space interactions as an important mechanism for spin-coupling in the S biradical **1**.

According to Hoffmann and coworkers,[15] through-bond coupling in **1S** involves the σ^* orbitals of bonds C2C3 and C5C6 (Fig. 2a), which overlap in a π-type fashion with the single electron orbitals and become partially occupied by the single electrons. This leads to a shortening of bonds C1C2, C3C4, C4C5, and C6C1, while bonds C2C3 and C5C6 are lengthened, as indicated in Figure 2a. In the T state, there is no through-bond electron

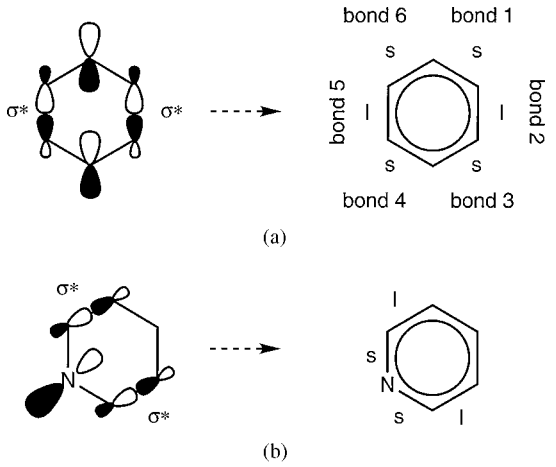

FIGURE 2. Spin-coupling mechanisms possible for biradicals **1S**–**7S**. (a) Through-bond interactions between the single electron orbitals involving the $\sigma^*(CC)$ orbitals of the HCCH fragments. (b) Anomeric delocalization of an N electron lone pair into the vicinal *CC* bonds. In each case, resulting changes in the bond lengths (l: longer; s: shorter) are indicated.

delocalization involving the single electrons (they cannot couple to occupy a σ^* orbital) and, therefore, the on-top density is larger in the σ regions of CC and CH bonds.

In summary, analysis of the on-top densities provides a better insight into the reliability of the UDFT description of a biradical such as **1S** than KS orbitals or spin densities do.[20, 24] Contrary to the spin densities, the on-top pair densities comply with the symmetry of the molecule both in the S and the T state. For the S state, the symmetry breaking leads to a twofold degenerate KS ground state, although the real ground state is not degenerate. Within the alternative interpretation of Perdew, Savin, and Burke,[24] these two ground states possess the same total and on-top pair density and, therefore, they are equivalent representations of the same KS ground state. The on-top pair densities for S and T state are very similar to each other, which is in line with the small energy difference between the two states, whereas the spin densities for the two states differ qualitatively from each other.

Symmetry breaking at the UDFT level fulfills the purpose of covering static correlation effects missing in restricted DFT and for the functional used. In calculations of typical multireference systems, the static correlation effects are formally covered as a part of the exchange energy.[20] The situation can be improved when DFT exchange is calibrated with the help of experimental data as is the case in hybrid functional theory.[25] Semiempirical DFT methods such as B3LYP[26] can be considered as methods designed to better cover static correlation effects (and, of course, lacking dynamic correlation effects) via the exchange functional. Hence, UDFT, and in particular UDFT, with hybrid functionals can provide a basis for a reasonable description of multireference systems with significant static electron correlation effects where this, of course, has to be verified from case to case. In this connection, we note that previous claims[12–14] pointing to a superior performance of the BLYP functional relative to the B3LYP hybrid functional in the case of the Bergman cyclization of the parent enediyne are not justified, because they were based on either (unstable) RDFT calculations[13, 14a, 14b] or the use of small basis set calculations as was recently shown by Gräfenstein and coworkers.[20]

DFT calculations show that **1S** is best described by UDFT using the B3LYP functional and a VTZP basis set. For example, the UB3LYP/6-311+G(3df,3pd) results for the energetic of the Bergman reaction of parent enediyne **8** are: activation enthalpy $\Delta H^{\ddagger}(470) = 30.9$ kcal/mol (exp. value at 470 K: 28.2[16]); reaction enthalpy $\Delta H_R(298) = 10.8$ (exp.: 8.5[16]) while the S-T splitting is 2.9 kcal/mol (exp.: 3.8[27]). Reasonable results (28.1, 4.3, and 2.7 kcal/mol) are also obtained with the 6-31G(d,p) basis set[28] and, therefore, this basis set is used throughout this work. For the verification of results, the 6-311+G(3df,3pd) basis[29] is employed only in single cases, because it has only little impact on calculated S-T splittings. The standard pruned (50,194) fine grid[30] was used, which is a reasonable compromise between calculational cost and accuracy. For each molecule investigated, geometry and vibrational frequencies were determined where the latter were used to verify local/global minimum character of the stationary points found in the geometry optimizations and to calculate zero-point energies (ZPE). Some of the molecules investigated turned out to be conformationally very flexible and, therefore, it was verified by analysis of the low frequency modes that the most stable conformation had been found. All calculations were performed with the *ab initio* programs COLOGNE 99[31] and GAUSSIAN 98.[32]

Structure and Stability of N-Containing Biradicals

Calculated energies of molecules **1**–**7** are listed in Table I, together with dipole moments, S-T splittings, and proton affinities (PA) relevant for the

TABLE I.
Absolute Energies, Zero-Point Energies ZPE, Frequencies ω_{low}, Dipole Moments μ, Singlet-Triplet Splittings $\Delta E(S-T)$, and Proton Affinities PA for Biradicals 1–7 at UB3LYP/6-31G(d,p).[a]

Biradical	Sym.	Energy	ZPE	ω_{low}	μ	$\Delta E(S-T)$	PA
1S	D_{2h}	−230.88193	46.6	413	0	2.5	
1T	D_{2h}	−230.87800	46.8	413	0		
2S	C_s	−246.93036	39.2	414	1.67	8.2	213.7
2T	C_s	−246.91723	39.6	352	2.10		219.1
3S	C_s	−247.27088	47.6	393	1.59	2.8	
3T	C_s	−247.26633	47.9	352	1.68		
4S	C_s	−361.46219	59.2	107	3.26	3.3	225.4
4T	C_s	−361.45685	59.6	89	3.48		227.2
5S	C_s	−361.82147	67.9	129	0.58	1.5	
5T	C_s	−361.81896	68.1	130	0.54		
6S	C_s	−341.57171	66.8	50	1.73	2.8	249.4
6T	C_s	−341.56731	67.1	23	1.95		250.4
7S	C_s	−341.96920	75.5	131	2.17	1.8	
7T	C_s	−341.96630	75.7	131	2.17		

[a] Energies in hartree, zero-point energies ZPE, singlet-triplet splittings, and proton affinities PA in kcal/mol, frequencies in cm^{-1}, and dipole moments in debye. ω_{low} denotes the lowest harmonic frequency calculated. The magnitude of ω_{low} indicates the conformational flexibility of the molecule in question, and verifies the minimum nature of the stationary point. Dipole moments of charged molecules are given with regard to a coordinate system based on the center of charge.

discussion of the stability of protonated enediynes. Table II summarizes energies for reference molecules **8**–**21**. In Figures 3 and 4, calculated geometries of S and T biradicals **1**–**7** are shown. Bond alternation of the S biradicals is analyzed in Table III utilizing calculated geometries of the T biradicals as a suitable reference. For all biradicals considered, the numbering of atoms shown in Scheme 1 for **1** is maintained, while for the numbering of bonds follows the convention given in Figure 2.

TABLE II.
Absolute Energies, Dipole Moments μ, and Proton Affinities PA for Molecules 8–21 at B3LYP/6-31G(d,p).[a]

Molecule	Sym.	Energy	μ	PA
8	C_{2v}	−230.88718	0.09	
9	C_s	−246.91554	2.32	217.2
10	C_s	−247.26161	1.23	
11	C_s	−361.47433	2.53	217.0
12	C_s	−361.82014	1.90	
13	C_s	−341.59097	1.19	240.0
14	C_s	−341.97347	2.85	
15	D_{6h}	−323.25821	0	
16	C_{2v}	−248.29261	2.18	235.6
17	C_s	−248.66807	1.87	
18	C_s	−362.84068	3.92	235.3
19	C_s	−363.21561	0.49	
20	C_s	−342.95017	2.38	258.0
21	C_s	−343.36128	2.09	

[a] Energies in hartree, dipole moments in debye, proton affinities PA in kcal/mol. Dipole moments of charged molecules are given with regard to a coordinate system based on the center of charge.

All biradicals investigated were optimized without any symmetry constraints, but turned out to be planar in the heavy atom part, converging to C_s symmetry within calculational accuracy. The abstraction of two H atoms from benzene (**15**) leads to a typical stretching of the benzene-hexagon and, by this, to reduced π-delocalization. Calculated geometries and S-T splittings of biradicals **1**, **2**, and **3** compare reasonably with those previously calculated by Cramer and Debbert,[12b] Cramer,[12c] and by Hoffner and coworkers[5] using DFT with the PW91 functional,[12] and CASSCF.[5, 12]

The degree of through-bond delocalization in S biradicals **1**–**7** is best assessed by comparing calculated lengths of the six-membered ring bonds with the corresponding values for the T states that do not benefit from through-bond delocalization of the single electrons. In Table III, calculated bond length differences ΔR_i (bond $i = 1,6$; see Table III) are listed in units of 10^{-3} Å for biradicals **1**–**7**. They are in line with the predicted bond variation pattern shown in Figure 2 for the two through-bond coupling mechanisms. Actually, the average ring

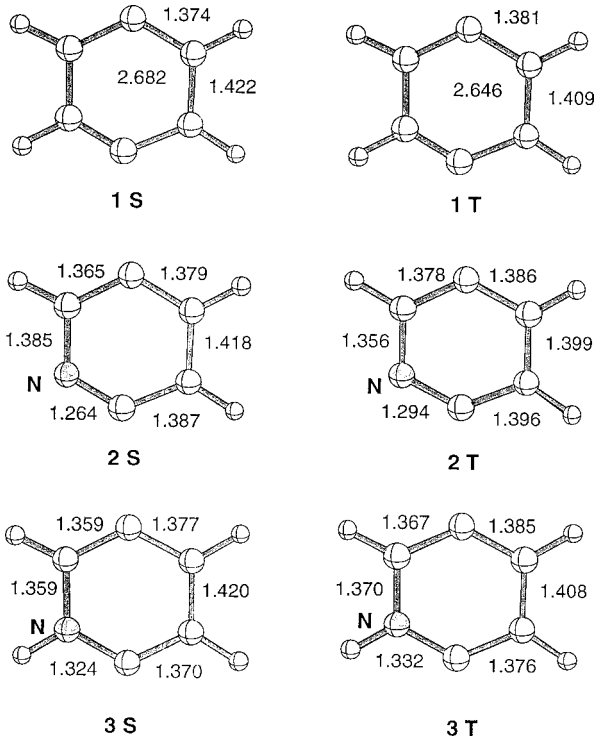

FIGURE 3. UB3LYP/6-31G(d,p) geometry of the S and T state of biradicals **1**, **2**, and **3**. Lengths in Å and angles in deg.

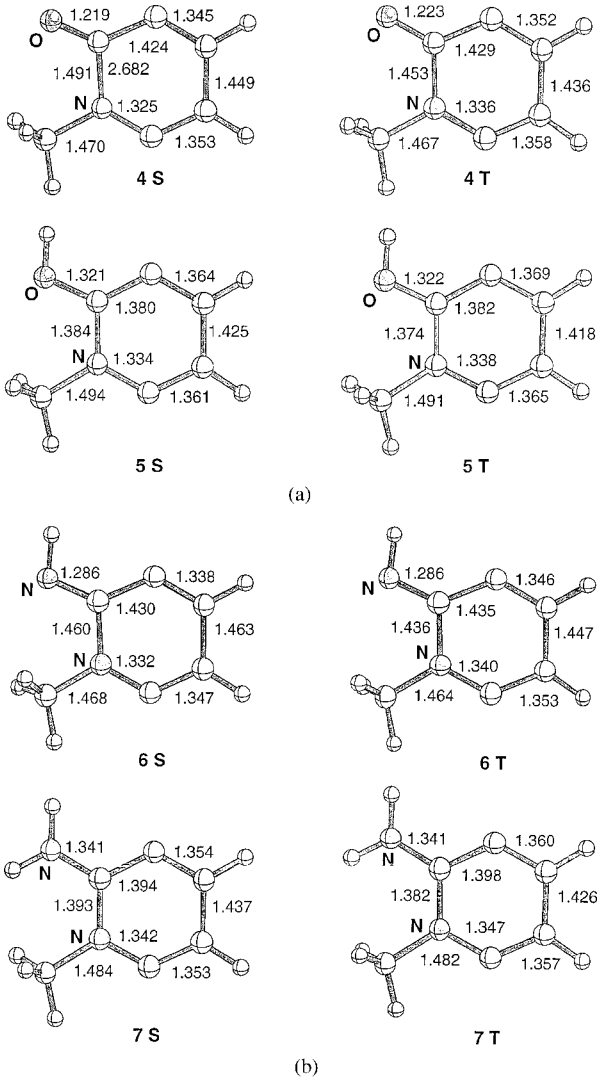

FIGURE 4. UB3LYP/6-31G(d,p) geometry of the S and T state of biradicals **4**, **5**, **6**, and **7**. Lengths in Å and angles in deg.

bond lengths R_{av} for all biradicals are almost identical for the T and S state. The increase in bond alternation found for the S state of **1** is exclusively due to through-bond coupling of the single electrons. Incorporation of an N atom in the ring of **1** increases bond alternation as reflected by the bond alternation parameter $\eta = (1/6)\sum_i^6 \Delta R_i$ (**1S**: $\eta = 9$; **2**: 21×10^{-3} Å, Table III). This suggests that the N atom supports through-bond interactions in line with the fact that the $\sigma^*(CN)$ orbital has a much lower energy than the $\sigma^*(CC)$ orbital because of the larger electronegativity of N. Also, orbital overlap between the interacting orbitals (Fig. 2a and 2b) is effectively increased due to the short CN bond length (1.264 Å; **1**: 1.381 Å, Fig. 3).

The length of the CN bond in **2S** has to be seen in connection with a second electronic effect, namely the anomeric delocalization of the in-plane N electron lone pair into vicinal CC bonds, which leads to the bond length pattern shown in Figure 2b and reflected by the bond lengths of **2T** in comparison with those of **3T**, for which anomeric delocalization is suppressed by protonation (see Fig. 3): The CN bonds of **2T** are much shorter than those of **3T**, while the vicinal CC bonds are much longer. The strongest effect is observed for bond C4N (bond 4), which also benefits from three-electron interactions involving the N lone pair electrons and the single electron at C4. Anomeric delocalization supports the through-bond coupling mechanism of the single electrons by shortening of the C4N bond and increasing orbital overlap. This is relevant for the stabilization of **2S**, because through-bond interactions will be particularly strong if either the overlap between the interacting orbitals is increased or the energy difference between the interacting orbitals is decreased. The larger electronegativity of the N atom guarantees that the $\sigma^*(C6N)$ orbital is lowered in energy, thus increasing through-bond interactions between the single electrons via the C6N

TABLE III.
Analysis of Through-Bond Interactions for Biradicals 1–7 (See Fig. 4).[a]

Mol.	Bond 1 C1C2	Bond 2 C2C3	Bond 3 C3C4	Bond 4 C4X	Bond 5 XC6	Bond 6 C6C1	η	R_{av}, **S**	R_{av}, **T**
1	−7	13	−7	−7	13	−7	9	1.390	1.390
2	−7	19	−9	−30	29	−13	18	1.366	1.368
3	−8	12	−6	−8	16	−8	10	1.373	1.373
4	−7	13	−5	−11	37	−5	13	1.398	1.394
5	−5	10	−4	−4	10	−2	6	1.375	1.374
6	−7	15	−4	−9	25	−5	11	1.393	1.393
7	−6	11	−4	−5	11	−4	7	1.379	1.378

[a] Bond length differences $\Delta R = R(S) - R(T)$ between T and S geometries are given in 10^{-3} Å. Bonds are numbered according to the numbering of the ring atoms (see Scheme 1). R_{av} denotes the average ring bond length for the S or T state. The bond alternation parameter η is given by (1/6) $\sum_i^6 |\Delta R_i|$ and is also given in units of 10^{-3} Å.

bond. At the same time, anomeric delocalization (two-electron effect) and three-electron delocalization lead to a shortening of the C4N bond and an increase in overlap.

This analysis is in line with discussions given by Cramer and Debbert,[12b] Cramer,[12c] and Hoffner and coworkers[5] as to the special role of N for the stabilization of **2S**, although the mechanism of stabilization was interpreted in these publications somewhat differently. Hoffner and coworkers[5] argue that N donates density to the antiperiplanar σ bonds in **2S** but withdraws density from these bonds in **3S** where they relate an increase (decrease) in density to stronger (weaker) through-bond coupling. This interpretation is misleading, because donation of electron density to the antiperiplanar σ bonds weakens rather than strengthens through-bond coupling. It is the anomeric (and the three-electron effect) on bond C4N, which is decisive for through-bond coupling and the strengthening of **2S** relative to **3S**. A change in inductive effects (N^+ is more electronegative than N), which would lead to a decrease in the electron density, does only play a minor role, as one can conclude by inspecting calculated geometries (Fig. 3). It should lead to a shortening of bonds C4N and NC5 (because of the smaller covalent radius of N^+ relative to N) and a lengthening of bond C3C4 if no other effects would be present. The net effect would be small, because changes would both increase and decrease through-bond coupling. Hence, it is actually the absence of anomeric delocalization in **3S**, which is decisive for the reduced through-bond coupling in this biradical.

The on-top density of aza-biradical **2S** reflects the strengthening of bonds C1C2, C4N, and C6C1. It extends relatively far into space at the side of the N electron lone pair and the sides of the C atoms with the single electrons (Fig. 5a). The difference on-top density of **2** (Fig. 5b) possesses a similar pattern of increase and decrease of P relative to the on top density of the T state. Distortions due the N lone pair and the three-electron interactions between electron lone pair and single electron are also obvious and in line with the analysis of bond length changes.

Biradical **2S** is 5.4 kcal/mol more stable than **1S**, as given by the energy of formal reaction (4) of Scheme 3 (see also Table IV). Three electronic effects will contribute to this energy: (1) difference in through-bond stabilization; (2) difference in anomeric stabilization for **2S** and formimine; (3) difference in resonance energies for **1S** and **2S**. The difference in S-T splittings suggests that 5.7 kcal/mol are due to the change in through-bond interactions. The difference in anomeric effects can be as large as 6 kcal/mol (difference PA(formimine) − PA(**2S**) = 219.7–213.7 kcal/mol), which requires a similarly large negative difference in resonance energies to get the value of 5.4 kcal/mol. Actually, the resonance energy of pyridine calculated at B3LYP/6-31G(d,p) (20.1 kcal/mol) with the help of the formal reaction

$$\text{pyridine} + 2CH_2{=}CH_2 + CH_2{=}NH \rightarrow \textit{trans}\text{-1-azabutadiene} + \textit{trans}\text{-butadiene} + \textit{trans}\text{-2-azabutadiene}$$

is 1.6 kcal/mol smaller than that of benzene (21.7 kcal/mol, see also ref. 33), which in total is 3.4 kcal/mol more stable than pyridine according to the energy of formal reaction (5) (Scheme 3 and Table IV). If one combines reaction (4) and the ref-

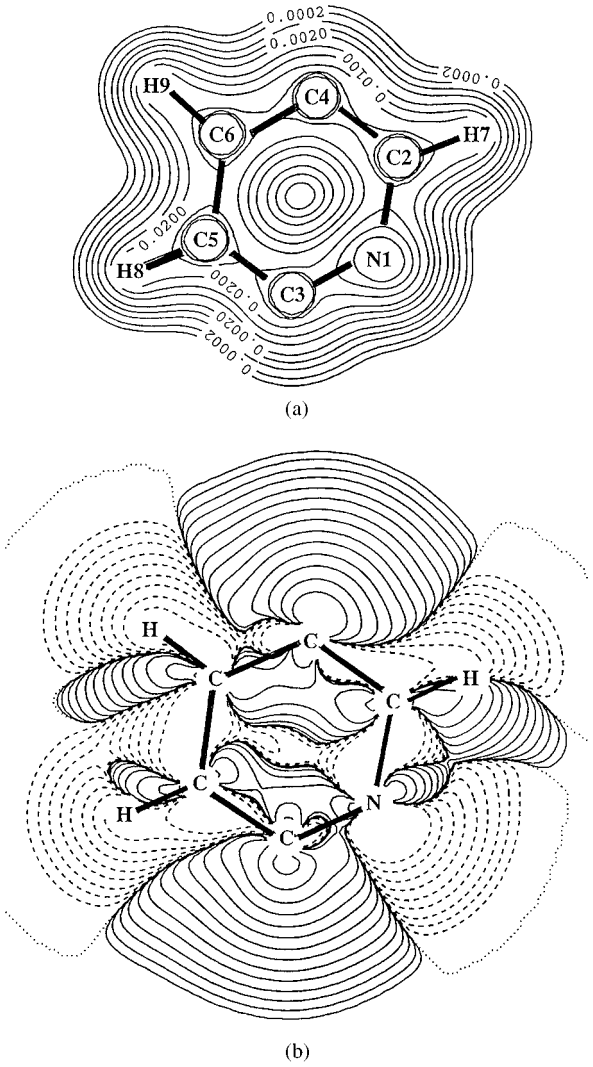

FIGURE 5. (a) UB3LYP/6-31G(d,p) on-top pair density distribution $P(\mathbf{r},\mathbf{r})$ given in form of a contur line diagram in the plane of *para*-didehydropyridine **2S**. (Contur lines: 0.0001, 0.0002, 0.0005, 0.001, 0.002, 0.005, 0.01, 0.02, 0.05, 0.1, 0.2 e/bohr^3). (b) Difference on-top density distribution $\Delta P(\mathbf{r},\mathbf{r}) = P(\mathbf{2S}) - P(\mathbf{2T})$ given in form of a contur line diagram in the plane of the molecule as calculated at the UB3LYP/6-31G(d,p) level of theory. Solid lines indicate a higher value for the S state, dashed lines, a higher value for the T state, the dotted line indicates equal values for both states. The UB3LYP/6-31G(d,p) geometry of **2S** was used. (Contur lines: 0, $\pm 3 \times 10^{-7}$, $\pm 10^{-6}$, $\pm 3 \times 10^{-6}$, $\pm 10^{-5}$, $\pm 3 \times 10^{-5}$, $\pm 10^{-4}$, $\pm 3 \times 10^{-4}$, $\pm 10^{-3}$ e/bohr^3).

erence reaction (5) to give reaction (6) ($\Delta_R E(4) - \Delta_R E(5) = \Delta_R E(6)$), the H abstraction ability of **2S** can be predicted to be 8.8 kcal/mol lower than that of **1S**, i.e., anomeric delocalization and through-bond coupling outweigh the decrease in resonance energy and stabilize **2S** so much that it becomes less reactive than **1S**.

Actually, the H abstraction ability of a biradical increases with its biradical character, which in turn, is reduced with increasing coupling between the single electrons of the biradical in its S state. Therefore, bond alternation in the S state as reflected by the parameter η gives direct insight into the stability of the S biradical, the magnitude of the S-T splitting, the biradical character and the H abstraction ability: The larger η is, the larger is the stability of the S state, the larger is the S-T splitting and the lower is the H abstraction ability. Clearly, **2S** possesses a lower H abstraction ability because of the anomeric delocalization of the N electron lone pair. This can only be increased by eliminating anomeric delocalization by N-protonation.

Protonation reduces through-bond coupling as is reflected by the geometry and the bond alternation parameter, which is for **3S** ($\eta(\mathbf{3S}) = 10$, Table III) slightly larger than for **1S** ($\eta(\mathbf{1S}) = 9$). Biradical **3S** is no longer stabilized relative to **1S** ($\Delta_R E(4) = -0.6$ kcal/mol, Table IV) and its S-T splitting is decreased from 8.2 (**2**) to 2.8 kcal/mol (**3**, Table I). Accordingly, **3S** should possess a similar (slightly smaller) H abstraction ability as **1S**. Nevertheless, the calculated $\Delta_R E(6)$ (−10.7 kcal/mol, Table IV) indicates that H abstraction by **3S** from benzene is clearly exothermic. The energy of reaction (6) reflects the thermodynamic situation, which is influenced by the fact that the resonance energy of protonated pyridine is larger than that of both benzene and pyridine: The value of $\Delta_R E(5)$ is 10.1 kcal/mol (Table IV) in line with strong stabilization of protonated pyridine.

In summary, the S-T splitting of **3** indicates that the kinetic ability of abstracting H atoms should be significantly larger for **2S** after protonation, but slightly lower than that of **1S**. Under thermodynamic control, biradical **3S** has a stronger H abstraction ability than **1S**. Protonation of the heteroatom increases the biradical character since it eliminates anomeric stabilization and reduces through-bond coupling (lengthening of the CN bond and reduction of overlap, Fig. 2). This is a wanted effect because protonation takes only place in the weakly acidic medium of the tumor cell where the biradical should become active in abstracting H atoms from the DNA of the tumor cell. It should be largely inactive (large S-T splitting) in the normal cell, in which protonation of **2S** cannot occur because of a pH value of 7.5. The question is only whether **2** is strong enough as a base to be protonated in tumor cells. The calculated PA value 214 kcal/mol (Table I)

TABLE IV.
B3LYP/6-31G(d,p) Energies $\Delta_R E$ for Formal Reactions (1), (3), (4), (5), and (6) shown in Scheme 3.[a]

Molecule	Description	Reac. (1)	Reac. (3)	Reac. (4)	Reac. (5)	Reac. (6)
2 or **16**	*Aza*	−9.3	12.6	5.4 (−0.3)	−3.4	8.8 (3.0)
3 or **17**	*Aza* − H^+	−5.8	9.1	−0.6 (−0.9)	10.1	−10.7 (−13.5)
4 or **18**	*Amide*	7.6	−4.3	−22.1 (−23.0)	−23.1	1.0 (−2.3)
5 or **19**	*Amide* − H^+	−0.8	4.1	−14.6 (−13.7)	−3.3	−11.2 (−10.4)
6 or **20**	*Amidine*	12.1	−8.8	−24.1 (−24.3)	−22.6	−1.4 (−1.7)
7 or **21**	*Amidine* − H^+	2.7	0.6	−22.8 (−21.0)	−12.9	−9.9 (−9.3)

[a] Reaction energies in kcal/mol. In the case of (4) and (6), the energies for the corresponding reactions involving the T biradicals are given in parentheses.

suggests that this may be questionable, although only the pK_A value can provide reliable information with regard to this question (see also refs. 5, 34, and 35, which provide discussions of the pK_A values for aza-enediynes).

Amide **4S** is strongly destabilized relative to **1S** ($\Delta_R E(4) = -22.1$ kcal/mol, Table IV) because the amide group weakens π-delocalization in the six-membered ring, also reflected by the CN bond length of 1.491 Å (Fig. 3) and the lengthening of R_{av} from 1.366 Å (**2S**, Table III) to 1.398 Å. Through-bond coupling is larger than in **1S**, but significantly smaller than in **2S** (η(**4S**) = 13, Table III), which corresponds to a S-T splitting of 3.3 kcal/mol (Table I). The biradical **4S** should have more biradical character than aza-biradical **2S**, but less than the parent biradical **1S**. Because amide **18** is 23.1 kcal/mol less stable than benzene (reaction 5, Table IV), the H transfer reaction (6) from benzene to biradical **4S** is only slightly endothermic by 1 kcal/mol.

Protonation of **4S** takes place at the O atom[36, 37] and reestablishes formally a 6π system (see Scheme 1) so that biradical **5S** is somewhat more stable than **4S** but still 14.6 kcal/mol less stable than **1S**, as indicated by the energy of reaction (4) (see Table IV). Similar as for aza-biradical **2**, protonation leads to a decrease of the S-T splitting (from 3.3 to 2.7 kcal/mol, Table I) thus indicating an increase in the biradical character of **5S**. Again, this increase is a result of geometrical changes caused by protonation (see Fig. 3): the length of bond NC6 decreases from 1.491 to 1.384 Å, which leads to a lowering of the energy of orbital $\sigma(NC)$ and a similar raise of the corresponding antibonding orbital that becomes less available for the through-bond coupling mechanism. Protonated amide **19** is 3.3 kcal/mol less stable than benzene (reaction 5, Table IV) so that H transfer from benzene to biradical **5S** becomes exothermic by −11.2 kcal/mol (reaction 6, Table IV).

Amidine biradical **6S** and its protonated counterpart **7S** possess similar properties as the amide biradicals **4S** and **5S** (Fig. 3, Tables III and IV). The calculated S-T splittings are 2.8 and 1.8 kcal/mol, respectively, in line with η values of 11 and 7 (Tables I and III). The biradical character increases with protonation and should be only slightly lower as in the case of the corresponding amides. Biradicals **6S** and **7S** are 24.1 and 22.8 kcal/mol less stable than the parent biradical **1S**, while the corresponding amidine **20** and amidinium ion **21** are 22.6 and 12.9 kcal/mol less stable than benzene (reaction 5, Table IV). Hence, the H transfer reaction (6) is exothermic by 1.4 and 0.9 kcal/mol, respectively (Table IV).

The basicity and the pK_A values of amidines are considerably higher than those of amides,[37] which is also reflected by the calculated PA values (**6S**: 249; **4S**: 225 kcal/mol, Table I). Even in the weakly acidic medium of the tumor cell amidine **6S** should be protonated to form **7S**, which has the higher biradical character and the larger H abstraction ability.

Chemical Relevance of Results

The biochemically active part of an enediyne is the biradical formed by the Bergman cycliza-

tion (1) of Scheme 1. Biradicals are more selective than radicals because of their smaller reactivity, as was discussed by Hoffner and coworkers.[5] Nevertheless, their reactivity must be high enough to abstract H atoms from a DNA molecule, which means that a compromise between selectivity and reactivity of a biradical must be found. It is beyond the scope of the present work to determine for a given enediyne this compromise because this would imply the investigation of H abstraction from a suitable model-DNA by enediyne with the help of quantum chemical calculations. Therefore, we follow Hoffner and coworkers,[5] and relate the reactivity of a biradical to its biradical character. The present work has shown that there is a clear connection between molecular geometry, the instability of a biradical, its S-T splitting, and its biradical character.

Through-bond interactions in **1S** depend on the availability of a relatively low-lying vicinal σ^* orbital, into which the single electrons of a S biradical can delocalize. Incorporation of an electronegative atom such as N into **1S** leads to a low-lying $\sigma^*(CN)$ orbital, and has also the effect of increasing overlap between the interacting orbitals (Fig. 2) because of a shorter CN distance. Anomeric delocalization of the N electron lone pair enhances through-bond interactions. This conclusion is in line with results for **1–3** obtained by other authors.[5, 12b, 12c]

The alternation of bond lengths in the S state (determined relative to the alternation of bond lengths in the T state) increases with increasing through-bond interactions. This is best measured by the bond alternation parameter η. The larger η and bond alternation is, the more stabilized is the S state. Stabilization of the S biradical leads to larger S-T splitting, which is a parameter that can be easily calculated for each biradical using UDFT.

Stabilization of the S biradical due to through-bond interactions and reflected by larger S-T splittings means stronger coupling of the single electrons and a reduction of both biradical character and the H abstraction ability.

The calculations presented in this work are the basis for the following conclusions.

1. Biradicals containing either the amide or amidine unit have S-T splittings comparable to that of the parent biradical **1S** (2–3 kcal/mol). Aza-biradicals such as **2S** have relatively large S-T splittings (about 8 kcal/mol) due to an increase of through-bond interactions by anomeric delocalization of the N electron lone pair. Therefore, they should not be suitable as H abstraction agents.
2. However, in all cases investigated, protonation leads to an increase in the biradical character and the H abstraction ability comparable or larger than that of the parent biradical. This is due to the fact that through-bond interactions are reduced (raising of the σ^* orbital). Because protonation can only take place in the weakly acidic medium of the tumor cell, N-containing biradicals are of interest in connection with the design of a new enediyne antitumor drug.
3. Calculated PA values indicate that both aza-biradical **2S** and amide biradical **4S**, which were discussed in connection with the design of new anti-tumor drugs,[5] are not suitable for this purpose, because they are too weakly basic to be protonated in the tumor cell. However, amidine **6S** should possess according to a PA value of 250 kcal/mol, a high enough basicity to guarantee protonation in the tumor cell.

Amidine biradicals can be formed by Bergman cyclization of the corresponding enediynes. We have investigated the enediynes related to the biradicals characterized in this work.[34] From the energies of reaction (1) and the corresponding barriers (see Table V) some predictions can be made with

TABLE V.
Reaction Barriers of the Bergman Cyclization of Various Enediynes.[a]

Enediyne	TS1a	Biradical	TS1b
8	31.2	3.2	28.0
9	21.8	−9.3	7.7
10	26.2	−5.8	20.0
11	28.8	7.6	2.9
12	28.2	−0.8	22.7
22	26.5	10.8	3.4
23	26.9	4.0	22.8
24	22.1	−1.9	22.3
13	29.4	12.1	7.2
14	28.6	2.7	20.6
25	25.1	13.5	5.6
26	27.8	7.5	19.8
27	19.0	5.4	5.8
28	21.2	−0.4	19.5

[a] Relative energies in kcal/mol obtained at the B3LYP/6-31G(d,p) level of theory.[35] TS1a and TS1b refer to the transition states of reactions 1a and 1b shown in Scheme 3.

regard to the possibility of generating biradicals from enediynes. The reaction energy of the Bergman cyclization of **8** is endothermic (3.2 kcal/mol), and possesses a barrier of 31.2 kcal/mol according to B3LYP/6-31G(d,p) calculations.[20] The corresponding values for the heteroenediyne/biradical systems listed in Table V are between −9.3 and 13.5 kcal/mol, and the corresponding barriers between 19.0 and 29.1 kcal/mol, respectively where also the ring systems **22–28** (Scheme 2) are considered. Amidine **13** and its protonated counterpart **14** cyclizise with relatively high barriers of about 29 kcal/mol, which is too high to lead to any significant biradical production at body temperature. However, incorporating the amidine into a 10-membered ring as in **25** leads to substantial lowering of the barrier (25.1 kcal/mol, Table V). Again, this effect is not sufficient to guarantee a fast reaction in the tumor cell because the barrier of protonated **25** (27.8 kcal/mol, Table V) would require reaction temperatures larger than 300 K to obtain a substantial yield of the corresponding biradical. One has to incorporate a double bond in the ten-membered ring as in **27** and **28** (thus increasing strain) to reduce barriers to a magnitude (19 and 21 kcal/mol) that guarantees Bergman cyclization at body temperature. The biradicals of **27** and **28** possess S-T splittings comparable to their parent molecules so that high biradical character and a strong H abstraction ability is guaranteed.

The biradicals associated with amidines **13**, **25**, and **27** easily undergo a retro-Bergman reaction (barriers: 5.6–7.2 kcal/mol, Table V) to isomeric compounds. However, this is a desirable effect, because the biradical concentration in the normal cell should be as low as possible. Protonation of amidine in the tumor cell leads to biradicals possessing barriers to retro-Bergman cyclization $\geq$20 kcal/mol (Table V), which increases their lifetime (protonation enhances their kinetic stability) and gives them a chance of abstracting H atoms from DNA and, by this, initiating death of the tumor cell. A more detailed description of the biochemical activity of amidines such as **13**, **14**, and their cyclic analogues is published elsewhere.[35]

To verify the results for amidine **6** and protonated amidine **7**, we repeated calculations at the UB3LYP/6-311+G(3df,3pd) level of theory. The calculated S-T splitting changes from 2.8 to 2.6 kcal/mol for the neutral molecule, while it does not change for the protonated species. In view of the accuracy obtained with UB3LYP/6-311+G(3df,3pd) for the parent biradical,[20] we conclude that results obtained in this work with the smaller basis are reasonable, and provide a basis for investigating enediynes with the amidine group in more detail.

Acknowledgments

This work was presented in part at the WATOC V Conference, London, 1999. We thank two unknown referees for useful and constructive comments. All calculations were done on the CRAY C90 of the Nationellt Superdatorcentrum (NSC), Linköping, Sweden. The authors thank the NSC for a generous allotment of computer time.

References

1. For reviews see (a) Borders, D. B.; Doyle, T. W., Eds. Enediyne Antibiotics as Antitumor Agents; Marcel Dekker: New York, 1995; (b) Nicolaou, K. C.; Smith, A. L. Acc Chem Res 1992, 25, 497; (c) Nicolaou, K. C.; Dai, W.-M. Angew Chem Int Ed Engl 1991, 30, 1387; (d) Pogozelski, W. K.; Tullius, T. D. Chem Rev 1998, 98, 1089; (e) Maier, M. E.; Boße, F.; Niestroj, A. J. Eur J Org Chem 1999, 1, 1; (f) Thorson, J. S.; Shen, B.; Whitwam, R. E.; Liu, W.; Li, Y.; Ahlert, J. Bioorgan Chem 1999, 27, 172; (g) Wisniewski Grimssom, J.; Gunawardena, G. U.; Klingberg, D.; Huang, D. Tetrahedron 1996, 19, 6453; (h) Fallis, A. G. Can J Chem 1999, 77, 159.
2. (a) Jones, R. R.; Bergman, R. G. J Am Chem Soc 1972, 94, 660; (b) Bergman, R. G. Acc Chem Res 1973, 6, 25; (c) Lockhart, T. P.; Comita, P. B.; Bergman, R. G. J Am Chem Soc 1981, 103, 4082; (d) Lockhart, T. P.; Bergman, R. G. J Am Chem Soc 1981, 103, 4091; (e) Gleiter, R.; Kratz, D. Angew Chem Int Ed Engl 1993, 32, 842; (f) Turro, N. J.; Evenzahav, A.; Nicolaou, K. C. Tetrahedron Lett 1994, 35, 8089; (g) Kuwatani, Y.; Ueda, I. Angew Chem Int Ed Engl 1995, 34, 1892.
3. See, for example, Casazza, A. M.; Kelly, S. L. In Borders, D. B.; Doyle, T. W., Eds. Enediyne Antibiotics as Antitumor Agents; Marcel Dekker: New York, 1995, p. 283.
4. (a) Tannock, I. F.; Rotin, D. Cancer Res 1989, 49, 4373; (b) Sevick, E. M.; Jain, R. K. Cancer Res 1988, 48, 1201.
5. Hoffner, J. H.; Schottelius, M. J.; Feichtinger, D.; Chen, P. J Am Chem Soc 1998, 120, 376.
6. Marquardt, R.; Balster, A.; Sander, W.; Kraka, E.; Cremer, D.; Radziszewiski, J. G. Angew Chem 1998, 110, 1001.
7. (a) David, W. M.; Kervin, S. M. J Am Chem Soc 1997, 119, 1464; (b) Chen, P. private communication.
8. Kraka, E.; Cremer, D. J Am Chem Soc 1994, 116, 4929.
9. Koga, N.; Morokuma, K. J Am Chem Soc 1991, 113, 1907.
10. (a) Wenthold, P. G.; Paulino, J. A.; Squires, R. R. J Am Chem Soc 1991, 113, 7414; (b) Wenthold, P. G.; Squires, R. R. J Am Chem Soc 1994, 116, 6401; (c) Wierschke, S. G.; Nash, J. J. Squires, R. R. J Am Chem Soc 1993, 115, 11958.
11. (a) Lindh, R.; Persson, B. J. J Am Chem Soc 1994, 116, 4963; (b) Lindh, R.; Lee, T. J.; Berhardsson, A.; Persson, B. J.; Karlstrm, G. J Am Chem Soc 1995, 117, 7186.
12. (a) Cramer, C. J.; Nash, J. J.; Squires, R. R. Chem Phys Lett 1997, 277, 311; (b) Cramer, C. J.; Debbert, S. Chem Phys Lett 1998, 287, 320; (c) Cramer, C. J. J Am Chem Soc 1998, 120,

6261; (d) Cramer, C. J.; Squires, R. R. Organic Lett 1999, 1, 215.

13. Chen, W.-C.; Chang, N.-Y.; Yu, C.-H. J Phys Chem A 1998, 102, 2484.
14. (a) Schreiner, P. R. J Am Chem Soc 1998, 120, 4184; (b) Schreiner, P. R. Chem Commun 1998, 483; (c) Schreiner, P. R.; Prall, M. J Am Chem Soc 1999, 121, 8615.
15. Hoffmann, R.; Imamura, A.; Hehre, W. J. J Am Chem Soc 1968, 90, 1499.
16. Roth, W. R.; Hopf, H.; Horn, C. Chem Ber 1994, 127, 1765.
17. Raghavachari, K.; Trucks, G. W.; Pople, J. A.; Head-Gordon, M. Chem Phys Lett 1989, 157, 479.
18. Handy, N. C.; Pople, J. A.; Head-Gordon, M.; Raghavachari, K.; Trucks, G. W. Chem Phys Lett 1989, 164, 185.
19. (a) Roos, B. O. In Advances in Chemistry & Physics, Vol. 69, Ab Initio Methods in Quantum Chemistry II; Lawley, K. P., Ed.; Wiley: New York, 1987, p. 447; (b) Andersson, K.; Malmqvist, P.-A.; Roos, B. O.; Sadlej, A. J.; Wolinski, K. J Phys Chem 1990, 94, 5483; (c) Andersson, K.; Malmqvist, P.-A.; Roos, B. O. J Phys Chem 1992, 96, 1218.
20. Gräfenstein, J.; Hjerpe, A. M.; Kraka, E.; Cremer, D. J Phys Chem 2000, 104, 1748.
21. Gräfenstein, J.; Cremer, D. to appear.
22. Noodleman, L.; Post, D.; Baerends, E. J. Chem Phys 1982, 64, 159.
23. (a) Ziegler, T.; Rauk, A.; Baerends, E. J. Theor Chim Acta 1977, 43, 261; (b) Noodleman, L.; Case, D. A. Adv Inorg Chem 1992, 38, 423; (c) Lovell, T.; McGrady, J. E.; Stranger, R.; MacGregor, S. Inorg Chem 1996, 35, 3079; (d) Ziegler, T.; Rauk, A.; Baerends, E. J. Theor Chim Acta 1997, 43, 261; (e) Cramer, C. J.; Dulles, F. J.; Giesen, D. J.; Almöff, J. Chem Phys Lett 1995, 245, 165.
24. Perdew, J. P.; Savin, A.; Burke, K. Phys Rev A 1995, 51, 4531.
25. (a) Becke, A. D. J Chem Phys 1993, 98, 5648. See also (b) Stevens, P. J.; Devlin, F. J.; Chablowski, C. F.; Frisch, M. J Phys Chem 1994, 98, 11623; (c) Becke, A. D. Phys Rev 1988, A38, 3098.
26. (a) See ref. 25; (b) Lee, C.; Yang, W.; Parr, R. G. Phys Rev 1988, B37, 785;
27. Wenthold, P. G.; Squires, R. R.; Lineberger, W. C. J Am Chem Soc 1998, 120, 5279.
28. Hariharan, P. C.; Pople, J. A. Theor Chim Acta 1973, 28, 213.
29. Krishnan, R.; Frisch, M.; Pople, J. A. Chem Phys 1980, 72, 4244.
30. Becke, A. D. J Chem Phys 1988, 88, 2547.
31. Kraka, E.; Gräfenstein, J.; Gauss, J.; Reichel, F.; Olsson, L.; Konkoli, Z.; He, Z.; Cremer, D. COLOGNE 99; Göteborg University: Göteborg, 1999.
32. Frisch, M. J.; Trucks, G. W.; Schlegel, H. B.; Scuseria, G. E.; Robb, M. A.; Cheeseman, J. R.; Zakrzewski, V. G.; Montgomery, J. A., Jr.; Stratmann, R. E.; Burant, J. C.; Dapprich, S.; Millam, J. M.; Daniels, A. D.; Kudin, K. N.; Strain, M. C.; Farkas, O.; Tomasi, J.; Barone, V.; Cossi, M.; Cammi, R.; Mennucci, B.; Pomelli, C.; Adamo, C.; Clifford, S.; Ochterski, J.; Petersson, G. A.; Ayala, P. Y.; Cui, Q.; Morokuma, K.; Malick, D. K.; Rabuck, A. D.; Raghavachari, K.; Foresman, J. B.; Cioslowski, J.; Ortiz, J. V.; Stefanov, B. B.; Liu, G.; Liashenko, A.; Piskorz, P.; Komaromi, I.; Gomperts, R.; Martin, R. L.; Fox, D. J.; Keith, T.; Al-Laham, M. A.; Peng, C. Y.; Nanayakkara, A.; Gonzalez, C.; Challacombe, M.; Gill, P. M. W.; Johnson, B.; Chen, W.; Wong, M. W.; Andres, J. L.; Gonzalez, C.; Head-Gordon, M.; Replogle, E. S. Pople, J. A. Gaussian 98, Revision A.3; Gaussian, Inc.: Pittsburgh, PA, 1998.
33. Minkin, V. I.; Glukhovtsev, M. N.; Simkin, B. Y. Aromaticity and Antiaromaticity, Electronic and Structural Aspects; Wiley: New York, 1994.
34. Kraka, E.; Cremer, D. J Mol Struct (Theochem) 2000, 506, 191.
35. Kraka, E.; Cremer, D. J Am Chem Soc 2000, 122, 8245.
36. (a) Zabicky, J., Ed. The Chemistry of Functional Groups, The Chemistry of Amides; Wiley: New York, 1970; (b) Homer, R. B.; Johnson, C. D. In Zabicky, J., Ed. The Chemistry of Functional Groups, The Chemistry of Amides; Wiley: New York, 1970, Chapt. 3.
37. Patai, S.; Rappoport, Z., Eds. The Chemistry of Functional Groups, The Chemistry of Amidines and Imidates; Wiley: New York, 1991; vol. 2.